Thermochimica Acta, 67 (1983) 361–376
Elsevier Science Publishers B.V., Amsterdam – Printed in The Netherlands

DETERMINATION OF KINETIC PARAMETERS OF THE DESORPTION OF PROPENE FROM A Re_2O_7/γ-Al_2O_3 CATALYST USING TEMPERATURE-PROGRAMMED DESORPTION

E.R.A. MATULEWICZ, B. SCHEFFER and J.C. MOL

Institute for Chemical Technology, University of Amsterdam, 1018 TV Amsterdam (The Netherlands)

(Received 21 March 1983)

ABSTRACT

The activation energy for desorption of propene from a metathesis catalyst has been determined using temperature-programmed desorption. Existing formulas for calculating the activation energy for desorption are extended, resulting in a new skilful method, which uses the half-width of the peak, and gives fast and accurate results.

NOTATION

A	frequency factor (s^{-1})
b	heating rate ($K\ s^{-1}$)
E	activation energy for desorption ($kJ\ mole^{-1}$)
E_2	exponential integral
F	flow rate of the carrier gas ($m^3\ s^{-1}$)
h	Planck constant (J s)
ΔH	adsorption enthalpy ($kJ\ mole^{-1}$)
k	Boltzmann constant ($J\ K^{-1}$)
k_i	rate constant for elementary process i ($s^{-1}\ kg^{-1}$)
n	order of desorption
p_a/p_0	relative pressure of the desorbing gas
r_i	rate of elementary process i ($m^3\ s^{-1}\ kg^{-1}$)
R	universal gas constant ($J\ mole^{-1}\ K^{-1}$)
ΔS_i	standard entropy change for elementary process i ($J\ mole^{-1}\ K^{-1}$)
$\Delta S^{\ddagger}$	activation entropy for desorption ($J\ mole^{-1}\ K^{-1}$)
t	time (s)
T	temperature (K)
T_{max}	temperature at maximum peak height (K)
$T_{1/2}^{+}$	temperature at half peak height for the high-temperature side of the peak (K)
$T_{1/2}^{-}$	temperature at half peak height for the low-temperature side of the peak (K)
v_m	volume of the reactant per unity of catalyst mass ($m^3\ kg^{-1}$)
W	mass of catalyst (kg)
θ	surface coverage of the catalyst

0040-6031/83/$03.00

INTRODUCTION

Temperature-programmed desorption (TPD) was first used by Amenomiya [1,2] as a means of understanding interactions between reactants and catalysts. By this method a reactant is desorbed from a catalyst surface in a stream of carrier gas, while the temperature of the catalyst is increased. Thus, various parameters, such as the activation energy and entropy for desorption, can be determined.

For a homogeneous catalyst surface the n-th order reaction rates for adsorption (r_a) and desorption (r_d) of the reactant are given by

$$r_a = Wv_m k_a \frac{p_a}{p_0}(1-\theta)^n \tag{1}$$

and

$$r_d = Wv_m k_d \theta^n \tag{2}$$

where W is the mass of the catalyst, v_m is the volume of the reactant that can adsorb on the catalyst per unity of mass, k_a and k_d are the rate constants for adsorption and desorption, p_a/p_0 is the relative pressure of the desorbed gas above the catalyst, and θ is the surface coverage of the catalyst.

From eqns. (1) and (2), a mass balance can be obtained

$$F\frac{p_a}{p_0} = Wv_m k_d \theta^n - Wv_m k_a \frac{p_a}{p_0}(1-\theta)^n \tag{3}$$

If no reaction takes place at the catalyst surface

$$F\frac{p_a}{p_0} = -Wv_m \frac{d\theta}{dt} \tag{4}$$

Substitution in eqn. (3) gives

$$-\frac{Wv_m b}{F}\frac{d\theta}{dT} = \frac{Wv_m k_d \theta^n}{F + Wv_m k_a (1-\theta)^n} \tag{5}$$

where F is the flow rate of the carrier gas, T is the temperature, and b is the heating rate. For desorption without readsorption, eqn. (5) becomes

$$-b\frac{d\theta}{dT} = k_d \theta^n = Ae^{-E/RT}\theta^n \tag{6}$$

This equation has been solved for $d\theta/dT$ at the temperature with maximum desorption rate and a homogeneous catalyst surface [3] to give

$$2\ln T_{max} - \ln b = \frac{E}{RT_{max}} + \ln\frac{E}{AR} - \ln n\theta_{max}^{n-1} \tag{7}$$

where E is the activation energy for desorption and A is the frequency

factor. For desorption with free readsorption [4,5] we get

$$2\ln T_{max} - \ln b = \frac{\Delta H}{RT_{max}} + \ln\left[\frac{(1-\theta_{max})^n W v_m \Delta H}{FR\exp(\Delta S/R)}\right] - \ln\left[\frac{n\theta_{max}}{1-\theta_{max}}\right]^{n-1} \quad (8)$$

where ΔH is the adsorption enthalpy and ΔS is the entropy loss. Equations (7) and (8) show that E or ΔH can be calculated by plotting $1/T_{max}$ vs. ($2\ln T_{max} - \ln b$), assuming that θ_{max} is independent of T_{max}. Another possibility for calculating E or ΔH is to assume that $A = 10^{13}\ s^{-1}$, so only one value of T_{max} would be required if n is known [6–9].

In this article we will describe a method for calculating the activation energy for desorption from the peak half-width. Moreover, we present results from TPD of propene from alumina and a $Re_2O_7/\gamma\text{-}Al_2O_3$ metathesis catalyst. The metathesis of propene is given by

$$2\ CH_2{=}CH{-}CH_3 \rightleftharpoons CH_2{=}CH_2 + CH_3{-}CH{=}CH{-}CH_3$$

EXPERIMENTAL

Figure 1 shows a flow diagram of the TPD system. The pressure, flow rate and temperature could be accurately controlled. Since the catalysts are very sensitive to impurities, a purification section was installed to remove water and oxygen from the carrier gas. The reactor itself was made of glass and placed in an electric oven. The flow rate was measured by thermal mass flow sensors. The temperature in the reactor was measured with calibrated chromel–alumel thermo-elements. The desorbed gas was detected by a flame ionization detector (FID), and identified by a mass spectrometer (MS).

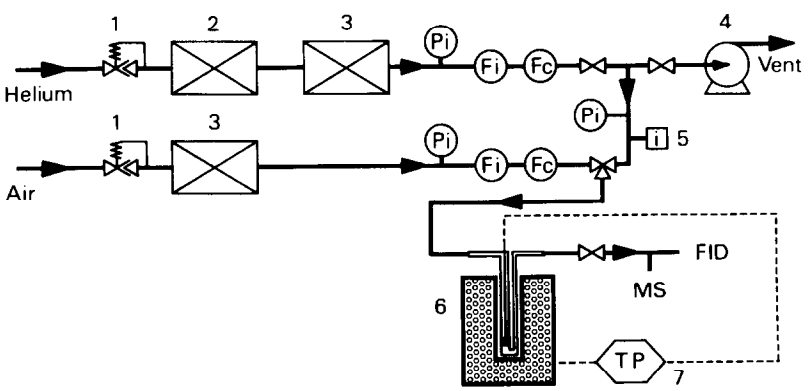

Fig. 1. Flow diagram of the TPD system. 1, Pressure controller; 2, column packed with Cu/Al_2O_3 catalyst (to remove oxygen); 3, column packed with molecular sieves (to remove water); 4, vacuum pump; 5, injection point; 6, oven and cooling unit with glass reactor; 7, temperature programming unit.

Catalyst samples with nominal Re_2O_7 contents of 6 and 18 wt.% were prepared by impregnation of γ-alumina (Ketjen CK-300, 180-230 μm, surface area 195 $m^2\ g^{-1}$ BET nitrogen) with an aqueous solution of ammonium perrhenate, followed by drying at 390 K and heating at 830 K in a stream of dry air.

The procedure for a TPD experiment was as described. The catalyst was activated in a stream of air at 820 K for 2 h, followed by a stream of helium at the same temperature for 2 h to remove the oxygen. After cooling under helium to 190 K, the system was evacuated and then propene was added. Subsequently, the catalyst was cooled to 77 K in a helium flow and the temperature-programmed heating of the catalyst was started at a chosen programming rate.

THEORY

When temperature-programmed desorption is described by the transition-state model, not only the activation energy for desorption is considered, but also the energy of the transition state. In the case of no readsorption, the adsorbed molecules are in equilibrium with the transition state.

Many investigators [6–9] assume that the frequency factor, A, in the Arrhenius equation is a constant, independent of the temperature, having a value of $10^{13}\ s^{-1}$ for unimolecular reactions in the gas phase [10]. However, A can change several orders of magnitute [10] and can be much less in the case of a negative $\Delta S^{\ddagger}$. If we compare Eyring's transition-state theory with the Arrhenius equation, it follows that A depends on the temperature: for a first-order desorption

$$A = \frac{kT}{h} \exp(\Delta S^{\ddagger}/R) \tag{9}$$

$\Delta S^{\ddagger}$ is built up from the internal entropy of the molecules (rotation, vibration) and the translational entropy [11]. Vibrational entropy is neglected. The activation entropy can be negative if during the formation of the transition state the decrease of the configuration and translational energy is larger than the increase of the internal entropy.

A theoretical calculation of the contributions of translation and rotation to the activation entropy for adsorbed propene yields a value of 123 J $mole^{-1}\ K^{-1}$ (a loss of two translations) and a value of 94 J $mole^{-1}\ K^{-1}$ (a loss of all rotations) when the transition state is considered to be immobile [12]. In our calculations, we assume that $\Delta S^{\ddagger}$ is constant for a TPD peak.

Now, we will discuss a new way of solving the equations for the desorption by means of measuring temperatures at maximal peak heights and at half peak heights.

For a first-order desorption without readsorption, integration of eqn. (6) gives

$$\ln \theta \Big|_{1}^{\theta_{T_1}} = -\int_0^{T_1} \frac{A}{b} \exp(-E/RT)\mathrm{d}T \tag{10}$$

or for $E/RT = x$

$$\ln \theta \Big|_{1}^{\theta_{T_1}} = -\int_{\infty}^{x_1} \frac{AE}{bR} \frac{\mathrm{e}^{-x}}{x^2}\mathrm{d}x = -\frac{AE}{bR}\int_{\infty}^{x_1} \frac{\mathrm{e}^{-x}}{x^2}\mathrm{d}x \tag{11}$$

Using the exponential integral [13]

$$\mathrm{E}_2(x) = x\int_x^{\infty} \frac{\mathrm{e}^{-t}}{t^2}\mathrm{d}t \tag{12}$$

eqn. (11) becomes

$$\ln \theta = -\frac{AE}{bR}\frac{\mathrm{E}_2(x)}{x} \quad \text{or} \quad \theta = \exp\left[-\frac{AE}{bR}\frac{\mathrm{E}_2(x)}{x}\right] \tag{13}$$

$\mathrm{d}\theta/\mathrm{d}T$ is coupled with $\mathrm{d}\theta/\mathrm{d}x$

$$\frac{\mathrm{d}\theta}{\mathrm{d}T} = \frac{R}{E}x^2\frac{\mathrm{d}\theta}{\mathrm{d}x} = -\frac{A}{b}\exp\left[-\frac{AE}{bR}\frac{\mathrm{E}_2(x)}{x} - x\right] \tag{14}$$

For the peak at half height we get

$$\left(\frac{\mathrm{d}\theta}{\mathrm{d}T}\right)_{1/2} = \frac{1}{2}\left(\frac{\mathrm{d}\theta}{\mathrm{d}T}\right)_{\max} \tag{15}$$

and substitution in eqn. (14) gives

$$\exp\left[-x_{\max}^2\,\mathrm{e}^{x_{\max}}\frac{\mathrm{E}_2(x_{1/2})}{x_{1/2}} - x_{1/2}\right] = \frac{1}{2}\exp\left[-x_{\max}^2\,\mathrm{e}^{x_{\max}}\frac{\mathrm{E}_2(x_{\max})}{x_{\max}} - x_{\max}\right] \tag{16}$$

After rearranging, we obtain

$$x_{\max}^2\,\mathrm{e}^{x_{\max}}\left[\frac{\mathrm{E}_2(x_{1/2})}{x_{1/2}} - \frac{\mathrm{E}_2(x_{\max})}{x_{\max}}\right] + x_{1/2} - x_{\max} = \ln 2 \tag{17}$$

There are two solutions for the peak at half height: one at a lower temperature ($T_{1/2}^-$) and one at a higher temperature ($T_{1/2}^+$) than the maximal peak height.

Assuming that

$$\frac{\mathrm{E}_2(x_{1/2}^-)}{x_{1/2}^-} \ll \frac{\mathrm{E}_2(x_{\max})}{x_{\max}} \quad \text{for } T_{1/2}^- < T_{\max} \tag{18}$$

and assuming that the approximation for $\mathrm{E}_2(x)$ for $x > 10$ is given by

$$\mathrm{E}_2(x) = \frac{\mathrm{e}^{-x}}{x} \tag{19}$$

eqn. (17) becomes

$$x_{1/2}^{-} - x_{max} = 1 + \ln 2 \tag{20}$$

and the expression for the activation energy becomes

$$E = \frac{(1 + \ln 2)R}{1/T_{1/2}^{-} - 1/T_{max}} = \frac{0.01401}{1/T_{1/2}^{-} - 1/T_{max}} \text{ (kJ mole}^{-1}\text{)} \tag{21}$$

Even though the assumptions may not be justified, the shape of eqn. (21) is useful [a linear relation between the activation energy and $(1/T_{1/2}^{-} - 1/T_{max})^{-1}$]. This relationship together with values of E calculated for $(1/T_{1/2}^{-} - 1/T_{max})$ from eqn. (17) give

$$E = \frac{0.0120}{1/T_{1/2}^{-} - 1/T_{max}} - 2.045 \text{ (kJ mole}^{-1}\text{)} \tag{22}$$

For the high-temperature part of the TPD peak, a similar expression can be derived

$$E = \frac{0.00786}{1/T_{max} - 1/T_{1/2}^{+}} - 1.685 \text{ (kJ mole}^{-1}\text{)} \tag{23}$$

For a second-order desorption without readsorption we can write

$$\frac{d\theta}{dT} = -\frac{A}{b} e^{-x} \left\{ \frac{1}{1 + [AE/Rb][E_2(x)/x]} \right\}^2 \tag{24}$$

For $y = -AE/Rb$ and $(d\theta/dT)_{1/2} = \frac{1}{2}(d\theta/dT)_{max}$, we obtain

$$e^{(x_{max} - x_{1/2})} \left\{ \frac{1 + y[E_2(x_{max})/x_{max}]}{1 + y[E_2(x_{1/2})/x_{1/2}]} \right\}^2 = 1/2 \tag{25}$$

Analogous procedures as in the case of the first-order desorption lead to

$$E = \frac{0.0143}{1/T_{1/2}^{-} - 1/T_{max}} - 2.539 \text{ (kJ mole}^{-1}\text{)} \tag{26}$$

and

$$E = \frac{0.0139}{1/T_{max} - 1/T_{1/2}^{+}} - 4.464 \text{ (kJ mole}^{-1}\text{)} \tag{27}$$

Equations (22), (23), (26) and (27) are given in Figs. 2, 3, 4 and 5, respectively. When E has been found, A can be calculated from

$$\frac{AE}{bR} = \frac{E^2}{R^2 T_{max}^2} e^{E/RT_{max}} \text{ (first order)} \tag{28}$$

$$\frac{AE}{bR} = \left(\frac{2 e^{-E/RT_{max}}}{(E/RT_{max})^2} - \frac{E_2(E/RT_{max})}{E/RT_{max}} \right)^{-1} \text{ (second order)} \tag{29}$$

The results from plotting (2 ln T_{max} − ln b) vs. $1/T_{max}$ [eqns. (7) and (8)] are often used for calculation of E and A. Here we will show that this method is not so reliable, especially not for calculation of A.

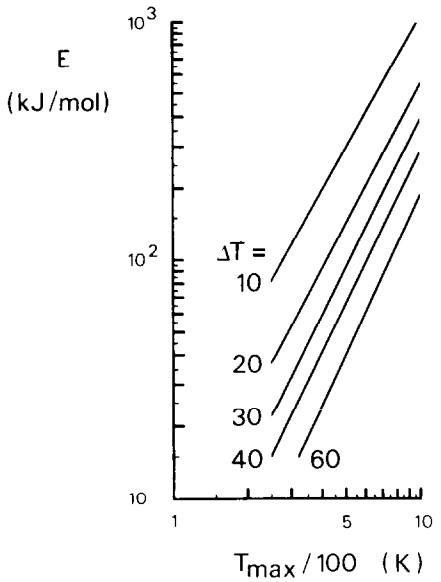

Fig. 2. Activation energy for a first-order desorption as a function of the maximum peak temperature for several values of $\Delta T = T_{max} - T_{1/2}^{-}$.

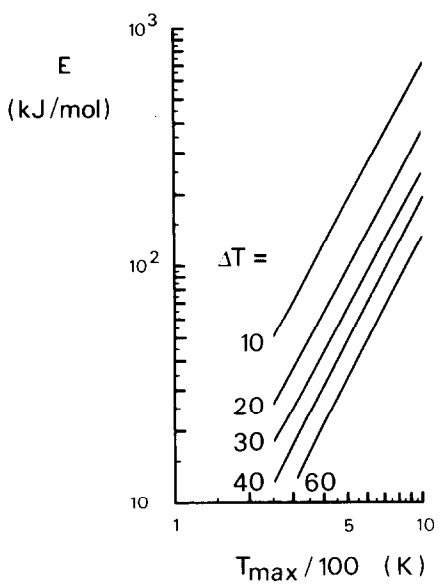

Fig. 3. Activation energy for a first-order desorption as a function of the maximum peak temperature for several values of $\Delta T = T_{1/2}^{+} - T_{max}$.

Developing ln T and $1/T$ as a Taylor series around temperature T_a, where $T = T_a + \Delta T$ gives

$$\ln(\Delta T + T_a) = \ln T_a + \frac{\Delta T}{T_a} - \frac{\Delta T^2}{2T_a} + \ldots \tag{30}$$

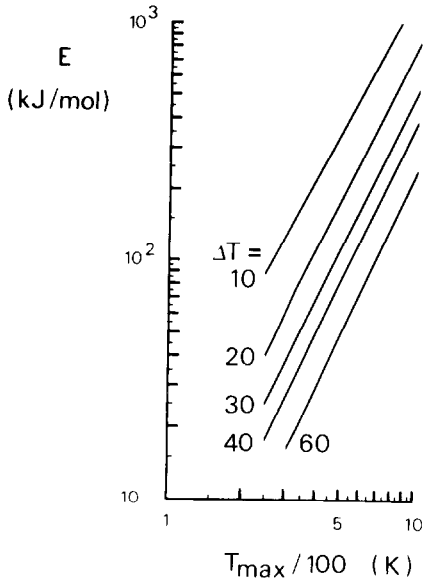

Fig. 4. Activation energy for a second-order desorption as a function of the maximum peak temperature for several values of $\Delta T = T_{max} - T^{-}_{1/2}$.

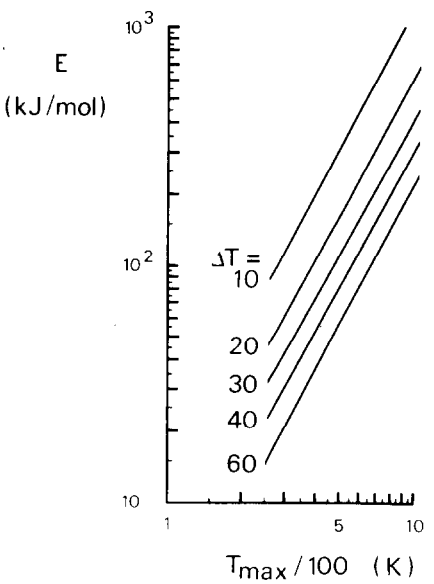

Fig. 5. Activation energy for a second-order desorption as a function of the maximum peak temperature for several values of $\Delta T = T^{+}_{1/2} - T_{max}$.

so

$$\ln T = \ln T_a + \frac{T}{T_a} - 1 + R_1(T) \tag{31}$$

and for $1/T$

$$\frac{1}{\Delta T + T_a} = \frac{1}{T_a} - \frac{\Delta T}{T_a^2} + \frac{\Delta T}{T_a^3} - \cdots \tag{32}$$

so

$$\frac{1}{T} = \frac{1}{T_a} - \frac{T}{T_a^2} + \frac{1}{T_a} + R_2(T) \tag{33}$$

Combining eqns. (31) and (33) gives

$$\ln T = T_a\left(\frac{1}{T}\right) + \ln T_a + 1 + R_3(T) \tag{34}$$

When $R_3(T)$ is small, $\ln T$ is linear with respect to $1/T$. For example, between 375 and 425 K the error is less than 0.5% if we linearize $\ln T$ with $1/T$. In many TPD studies, a plot of $1/T$ vs. $\ln T$ gives a good fit, but only E can be determined satisfactorily. It should be noted, however, that the goodness of the fit is sometimes overvalued because the mathematical correlation between $1/T$ and $\ln T$ is neglected.

For first-order processes Grosswiener [14] deduced an empirical formula from the thermoluminiscence (glow curves): this has been corrected by Dussel and Bube [15], such that it resembles the formulas shown before [eqns. (22) and (26)], i.e.

$$E = 1.41\frac{kT_{max}T_{1/2}^-}{T_{max} - T_{1/2}^-} \text{ (eV)} \tag{35}$$

and for second-order processes

$$E = 1.68\frac{kT_{max}T_{1/2}^-}{T_{max} - T_{1/2}^-} \text{ (eV)} \tag{36}$$

Chen [16] also presented an empirical relation for a first-order process

$$E = 1.52\frac{kT_{max}^2}{T_{max} - T_{1/2}^-} - 1.58(2kT_{max}) \text{ (eV)} \tag{37}$$

and for a second-order process

$$E = 1.813\frac{kT_{max}^2}{T_{max} - T_{1/2}^-} - 2(2kT_{max}) \text{ (eV)} \tag{38}$$

For the high-temperature part of the peak, similar formulas were given. In Table 1 the formulas for glow curves in the thermoluminiscence as well as formulas derived in this paper are used for the calculation of E from

TABLE 1

The activation energy of desorption calculated by several methods, compared with the theoretical values for different temperatures and half peak widths

T_{max}	$T^{-}_{1/2}$	E, first order (kJ mole^{-1})				E, second order (kJ mole^{-1})			
		Theoretical	Eqns. (22),(23)	Grosswiener	Chen	Theoretical	Eqns. (26),(27)	Grosswiener	Chen
300	240	12.72	12.4	14.1	11.1	14.37	14.6	16.8	12.6
400	385	122.09	121.3	121.3	124.2	145.64	144.3	143.3	147.4
500	480	142.50	142.1	140.6	144.8	169.85	169.1	167.5	171.7
650	625	193.14	193.2	190.4	196.4	230.33	229.8	226.9	232.6
700	660	135.74	136.7	135.3	136.4	160.94	162.6	161.2	161.3
	$T^{+}_{1/2}$								
300	360	12.48	12.5		12.2	20.69	20.6		21.3
300	340	18.48	18.4		18.3	31.46	31.1		31.9
500	540	51.00	51.4		50.7	88.71	89.5		88.6
700	740	99.87	100.1		99.4	175.30	175.3		173.7

theoretical TPD curves and compared with the theoretical values of E. Equations (22), (23), (26) and (27) give especially good results over a broad temperature range. Moreover, Figs. 4–7, which are the graphical representation of these formulas, can serve as reference charts for a fast determination of the activation energy for desorption. Only one TPD experiment is necessary if the order of desorption is known: on the other hand, if the order is not known it can be determined by using the half-widths for both the low and high temperature sides of the peak, which, for the right order, must give the same value for the activation energy for desorption.

EXPERIMENTAL

Temperature-programmed desorption of propene

γ-Al_2O_3

Different amounts of propene were added to the alumina. At a heating rate of 8.1 K min^{-1}, a primary peak is seen at about 510 K, which shifts to a higher temperature if the amount of propene decreases (Fig. 6). The second peak, occurring at about 625 K, results from the dimerization of propene on the alumina. This peak decreases with decreasing amount of adsorbed propene, and with increasing heating rate. The dimer peak is only found on pure alumina.

Re_2O_7 on γ-Al_2O_3

For catalysts with 6 and 18 wt.% Re_2O_7, the TPD spectra were recorded with different heating rates and with different amounts of adsorbed propene.

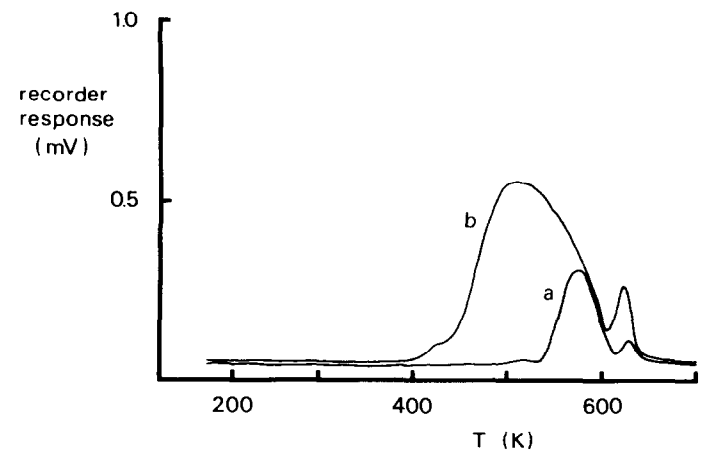

Fig. 6. Desorption spectrum of propene on Al_2O_3. Heating rate = 8.1 K min^{-1}. Propene added: a, 0.6 μmole; b, 3 μmole.

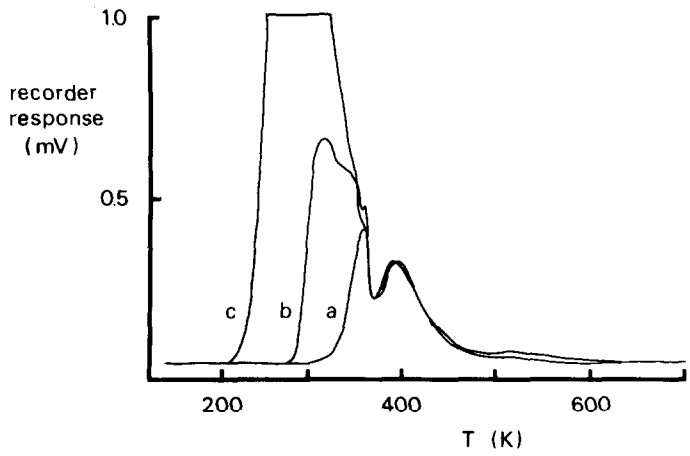

Fig. 7. Desorption spectrum of propene on a 18 wt.% $Re_2O_7/\gamma\text{-}Al_2O_3$ catalyst. Heating rate = 8.1 K min^{-1}. Amount of propene added (μmole): a, 0.2; b, 0.6; c, 4.

Figure 7 shows the influence of the amount of adsorbed propene on an 18 wt.% $Re_2O_7/\gamma\text{-}Al_2O_3$ catalyst. Two different peaks can be observed: one below 370 K, whose intensity increases with increasing amount of adsorbed propene, and one at about 390 K, which is independent of the amount of adsorbed propene. The same picture is obtained with a 6 wt.% catalyst. Figure 8 shows the TPD spectrum for the pure alumina (a) and for the 6 and 18 wt.% $Re_2O_7/\gamma\text{-}Al_2O_3$ catalysts (b and c), all at the same heating rate (8.1 K min^{-1}). Only the Re_2O_7-containing catalysts show two adsorption peaks for propene, whereas the alumina shows only one propene peak besides the

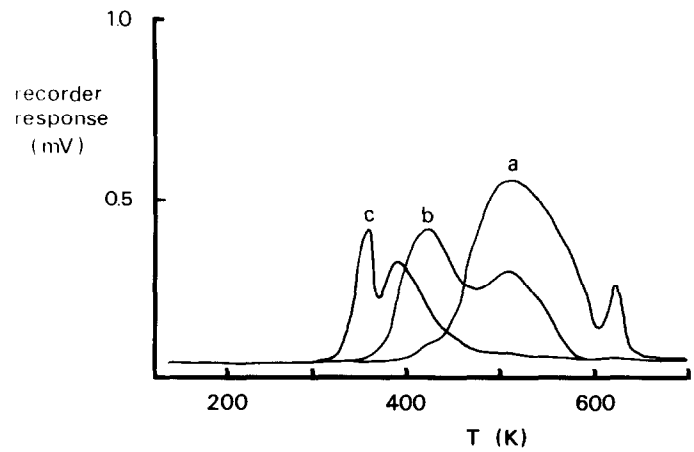

Fig. 8. Desorption spectrum of propene on: a, Al_2O_3, 3 μmole propene added; b, 6 wt.% $Re_2O_7/\gamma\text{-}Al_2O_3$, 0.6 μmole propene added; c, 18 wt.% $Re_2O_7/\gamma\text{-}Al_2O_3$, 0.2 μmole propene added. Heating rate = 8.1 K min^{-1}.

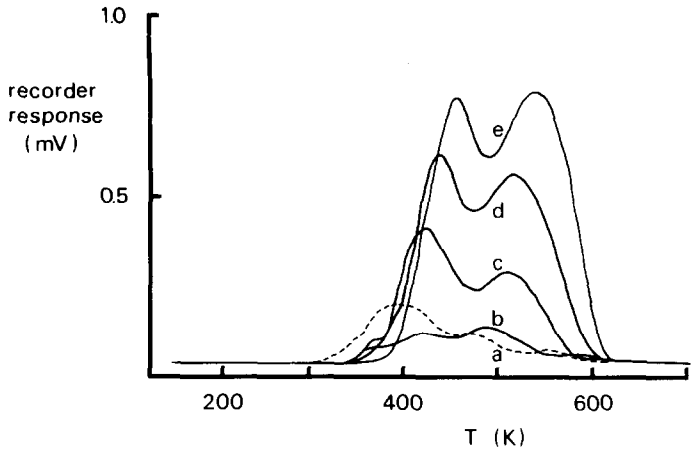

Fig. 9. Desorption of propene on a 6 wt.% Re_2O_7/γ-Al_2O_3 catalyst with 0.6 μmole of propene added. Heating rates (K min^{-1}): a, 1.6 (recorder response × 2); b, 3.2; c, 8.1; d, 15.8; e, 26.6.

dimer peak. Figure 9 shows the TPD spectrum for the 6 wt.% Re_2O_7/γ-Al_2O_3 catalyst; here the heating rate is varied and the adsorbed amount of propene is kept constant. With increasing heating rate, T_{max} shifts to higher temperatures.

DISCUSSION

The shift of the peak maximum with increasing amount of adsorbed propene on the pure alumina shows that the surface of the alumina is heterogeneous with respect to propene adsorption. When small amounts of propene are added, the adsorption sites with the highest desorption temperature (strongest adsorption) are occupied first. As our model is only valid for homogeneous surfaces, it is not possible to calculate the activation energy of desorption in this case. The formation of the dimer only occurs on the alumina.

From data published by Kapteyn [12] we could calculate that the readsorption of propene under our experimental conditions can be neglected compared with desorption. From Fig. 7 it is clear that adding too much propene disturbs the TPD spectrum. This can be attributed to physical adsorption of the propene, i.e. the peak below 370 K. To lower this influence, only small amounts of propene were added to the catalyst, but, for example, for the 18 wt.% Re_2O_7/γ-Al_2O_3 the physically adsorbed propene is still present (Fig. 8).

According to the literature, a monolayer of Re_2O_7 will be formed on the catalyst during calcination for Re_2O_7 loadings smaller than about 18 wt.%

[18,19]. For the 6 wt.% loading, the alumina is not completely covered with Re_2O_7 and adsorption of propene on alumina is still possible. Therefore, the peak at about 510 K in curve b of Fig. 8 is attributed to adsorbed propene on alumina. Because of the heterogeneity of the alumina, the activation energy is not calculated.

Both the peak at about 420 K (curve b) of the 6 wt.% catalyst and the peak at about 390 K for the 18 wt.% catalyst (curve c) are contributed to by propene desorption from the Re_2O_7. At higher Re_2O_7 contents the peak shifts to lower desorption temperatures and thus corresponds with a lower activation energy of desorption.

In Table 2 the desorption activation energy calculated with the formulas postulated here is compared with the $(2\ln T_{max} - \ln b)$ vs. $1/T_{max}$ method. Table 2 shows hardly any difference between the different methods used; in the case of the $(2\ln T_{max} - \ln b)$ vs. $1/T_{max}$ method, more experiments are required than for the half-width method to get reliable results.

Figure 10 compares, as a typical example, the peak calculated with eqn. (14) with the measured peak. Because of the disturbance of the adsorption on alumina for the 6 wt.% Re_2O_7-catalyst, we have fitted a first-order desorption for the second peak. The figure shows good agreement between the values calculated with our model and the experimental results.

The values for the activation entropy for desorption are in good agree-

TABLE 2

Values for the activation energy of desorption of propene and the entropy, calculated for the 6 wt. % and the 18 wt. % Re_2O_7/γ-Al_2O_3 catalyst

b	T_{max}	Half peak width method				$(2\ln T_{max} - \ln b)$ vs. $1/T_{max}$ method	
		$T_{1/2}$	E (kJ mole^{-1})	A (s^{-1})	$\Delta S^{\ddagger}$ (J mole^{-1} K^{-1})		
6 wt. % Re_2O_7/γ-Al_2O_3							
1.6	391	361	54.5	2.2×10^4	−179		
3.2	418	390	67.9	7.6×10^5	−150	E	$= 63.6$ kJ mole^{-1}
8.1	424	396	70.0	2.7×10^6	−140	A	$= 3.5\times10^5$ s^{-1}
15.8	437	406	66.7	1.0×10^6	−148	$\Delta S^{\ddagger}$	$= -156$ J mole^{-1} K^{-1}
26.6	453	419	65.0	5.3×10^5	−154		
18 wt. % Re_2O_7/γ-Al_2O_3							
1.6	317	337	36.0	952	−204		
3.1	352	378	34.5	227	−216	E	$= 22.9$ kJ mole^{-1}
8.1	393	427	33.2	89	−225	A	$= 223$ s^{-1}
16.9	415	448	38.1	467	−212	$\Delta S^{\ddagger}$	$= -217$ J mole^{-1} K^{-1}
25.6	416	450	37.2	517	−211		

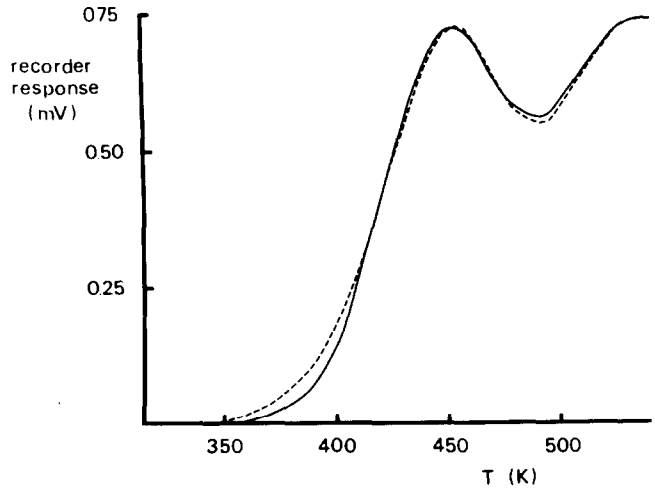

Fig. 10. Typical recorded TPD spectrum (————) compared with the calculated (· · · · · ·) curve for a 6 wt.% Re_2O_7/γ-Al_2O_3 catalyst.

ment with the value reported by Kapteyn [12] for the overall metathesis of propene on a Re_2O_7/γ-Al_2O_3 catalyst. The values of -156 and -217 J $mole^{-1}$ K^{-1} for $\Delta S^{\ddagger}$ (Table 2) are very close to Kapteyn's theoretically predicted value, i.e. between -123 and -217 J $mole^{-1}$ K^{-1}. For the 6 wt.% Re_2O_7 content, $\Delta S^{\ddagger}$ for propene in the transition state corresponds with the theoretical translational entropy and for the 18 wt.% Re_2O_7 content with both the translational and rotational entropy.

The amount of adsorbed propene is very small; propene is adsorbed on only 0.2% of the Re_2O_7 of the 18 wt.% Re_2O_7/γ-Al_2O_3 catalyst: for the 6 wt.% catalyst, propene is adsorbed on only 1%. This is in agreement with data for the number of rhenium atoms that are catalytically active which have been reported for a similar catalyst. From NO adsorption experiments, this number was established to be less than 0.3% [20], while calculated values from a kinetic study of the metathesis of propene resulted in less than 1% [17].

Kapteyn [12] observed that the initial reaction rate for the metathesis of propene increases sharply as a function of the Re_2O_7 content of the catalyst. Two different areas were observed: below about 6 wt.% Re_2O_7 the reaction rate is almost linear as a function of the Re_2O_7 content, whereas above about 10% Re_2O_7 the reaction rate is proportional to a higher power of the Re_2O_7 content. It seems, therefore, that with increasing Re_2O_7 content the nature of the catalyst is changing, as is also shown by the peak temperature shift in the TPD spectra (Fig. 8). In this respect, it is noted that Nakamura et al. [21] suggested that the low-loading Re_2O_7/γ-Al_2O_3 metathesis catalysts have only monomeric surface rhenium species, and the high-loading catalysts have ligated dimeric rhenium species as the active sites.

REFERENCES

1 Y. Amenomiya and R.J. Cvetanović, J. Phys. Chem., 67 (1963) 144.
2 Y. Amenomiya, Chemtech, (1976) 128.
3 F.M. Lord and J.S. Kittelberger, Surf. Sci., 43 (1974) 173.
4 J.A. Konvalinka, J.J.F. Scholten and J.C. Rasser, J. Catal., 48 (1977) 365.
5 R.J. Cvetanović and Y. Amenomiya, Adv. Catal., 17 (1967) 103.
6 G.G. Low and A.T. Bell, J. Catal., 57 (1979) 397.
7 M. Bowker, H. Houghton and K.C. Waugh, J. Chem. Soc. Faraday Trans. 1, 77 (1981) 3023.
8 K. Kawasaki, M. Shibata, H. Miki and T. Kioka, Surf. Sci., 81 (1979) 370.
9 R.G. Donnelly, M. Modell and R.F. Baddour, J. Catal., 52 (1978) 239.
10 R.C. Baetzhold and G.A. Somorjai, J. Catal., 45 (1976) 94.
11 S.W. Benson, Thermochemical Kinetics, Wiley, New York, 2nd edn., 1976.
12 F. Kapteyn, Ph.D. Thesis, University of Amsterdam, 1980.
13 M. Abramowitz and I.A. Stegun, Handbook of Mathematical Functions, Dover Publications, New York, 1965.
14 L.I. Grosswiener, J. Appl. Phys., 24 (1953) 1306.
15 G.A. Dussel and R.H. Bube, Phys. Rev., 155 (1967) 764.
16 R. Chen, J. Appl. Phys., 40 (1969) 570.
17 F. Kapteyn, L.H.G. Bredt, E. Homburg and J.C. Mol, Ind. Eng. Chem. Prod. Res. Dev., 20 (1981) 457.
18 A.A. Olsthoorn and C. Boelhouwer, J. Catal., 44 (1976) 197.
19 F. Kapteyn, L.H.G. Bredt and J.C. Mol, Recl. Trav. Chim. Pays-Bas, 96 (1977) M139.
20 A.A. Olsthoorn and C. Boelhouwer, J. Catal., 44 (1976) 207.
21 R. Nakamura, F. Abe and E. Echigoya, Chem. Lett., (1981) 51.